Thermosensitive Nanospheres with a Gold Layer Revealed as Low-Cytotoxic Drug Vehicles

ARTICLE *in* LANGMUIR · OCTOBER 2005

Impact Factor: 4.46 · DOI: 10.1021/la051069t · Source: PubMed

Thermosensitive Nanospheres with a Gold Layer Revealed as Low-Cytotoxic Drug Vehicles

Jian Qin,[†] Yun Suk Jo,*[,‡] Jong Eun Ihm,[‡] Do Kyung Kim,[†,§] and Mamoun Muhammed*[,†]

Materials Chemistry Division, Royal Institute of Technology, Stockholm SE-100 44, Sweden, Integrative Biosciences Institute (IBI), École Polytechnique Fédérale de Lausanne (EPFL), Lausanne CH 1015, Switzerland, and Institute of Science and Technology in Medicine, Keele University, Thronburrow Drive, Hartshill, Stoke-on-Trent, ST4 7QB, United Kingdom

Received April 21, 2005. In Final Form: July 10, 2005

In this paper, the positive effect of a gold layer on cell viability is demonstrated by examining the results given by 3-(4,5-dimethylthiazol-2-yl)-5-(3-carboxymethoxyphenyl)-2-(4-sulfop henyl)-2*H*-tetrazolium (MTS) assay and two-color cell fluorescence viability (TCCV) assay. These cytotoxicity tests were performed with human cervical adenocarcinoma cells (HeLa cell line) and transformed African green monkey kidney fibroblast cells (Cos-7 cell line). To fabricate the nanostructures as drug vehicles, first, poly(L,L-lactide-*co*-ethylene glycol) (PLLA-PEG) and poly(*N*-isopropylacrylamide-*co*-D,D-lactide) (PNIPAAm-PDLA) were synthesized, and then two kinds of thermosensitive nanospheres comprising "shell-in-shell" structures without a gold layer (PLLA-PEG@PNIPAAm-PDLA) and with a gold layer (Au@PLLA-PEG@PNIPAAm-PDLA) were constructed by a modified double-emulsion method (MDEM). Both of them displayed a unique thermosensitive character exhibiting the lower critical solubility temperature (LCST) at 36.7 °C which was confirmed by UV−vis spectroscopy and differential scanning calorimetry (DSC). The release profiles of entrapped bovine serum albumin (BSA) were monitored at 22 and 37 °C, respectively, to reveal the thermal dependence on the release rate. In cell viability tests, both PLLA-PEG@PNIPAAm-PDLA and Au@PLLA-PEG@PNIPAAm-PDLA showed excellent cell viability, and furthermore, Au@PLLA-PEG@PNIPAAm-PDLA, particularly at high doses, exhibited more enhanced cell viability than PLLA-PEG@PNIPAAm-PDLA. This effect is mainly attributed to the gold layer which binds the protein molecules first and consequently facilitates transmembrane uptake of essential nutrients in the cell media, resulting in favorable cell proliferation.

1. Introduction

Elemental gold is known as one of the most biocompatible materials due to its chemical inertness. Recently, considerable attention has been given to the development of novel biomedical applications of gold.[1,2] Gold has been applied widely as a prosthetic in surgery or dentistry.[3,4] In 1980, immunogold staining was first advocated by De Mey et al. and became one of the earliest applications of the colloidal gold particles in the past two decades.[5−12] Surface-modified colloidal gold can be utilized as biosensors,[13,14] and dielectric nanoparticles enclosed with a gold shell have been applied in the tumor therapy utilizing the absorption of near-infrared (NIR) light.[15] Moreover, gold-related polynucleotide and DNA analysis,[16,17] gene delivery,[18] modulated drug delivery,[19] and the investigation of cell biology[20] are also fueling a variety of bio-inspired scientific fields. Although many biomedical applications of gold nanoparticles have been developed, the detrimental effects of such nanoparticles have been overlooked. Though recent analysis has indicated that colloidal gold does not cause acute cytotoxicity, it is believed that the nanoparticles could be rapidly modified by the surrounding cellular environment.[21] This process could, in turn, potentially alter the properties of the substrates such as nanoparticles, and the present hypothesis clearly implies that proteins would attach to the surface of the gold layer and regulate the interactions between the nanospheres and cellular membranes.

Drug delivery systems (DDS) have been designed to improve the pharmacological and therapeutic properties of drugs compared to the conventional free drugs.[22] The

* To whom correspondence should be addressed. E-mail: yunsuk.jo@epfl.ch; mamoun@mse.kth.se. Phone: +41 21 693 1733 (Y.S.J.); +46 8 790 8158 (M.M.). Fax: +41 21 693 9690 (Y.S.J.); +46 8 790 9072 (M.M.).

† Royal Institute of Technology.

‡ École Polytechnique Fédérale de Lausanne (EPFL).

§ Keele University.

(1) Merchant, B. *Biologicals* **1998**, *26*, 49.
(2) Katz, E.; Willner, I. *Angew. Chem., Int. Ed.* **2004**, *43*, 6042.
(3) Levison, D. A.; Crocker, P. R.; Lee, G.; Shepherd, N. A.; Smith, A. P. *J. Pathol.* **1984**, *144*, 119.
(4) Jobe, R. *Plast. Reconstr. Surg.* **1993**, *91*, 563.
(5) De Mey, J.; Moeremans, M.; Geuens, S.; Nuydens, R.; Vanbelle, H.; Debrabander, M. *Eur. J. Cell Biol.* **1980**, *22*, 297.
(6) Moeremans, M.; Daneels, G.; Vandijck, A.; Langanger, G.; De Mey, J. *J. Immunol. Methods* **1984**, *74*, 353.
(7) Ma, Z. F.; Sui, S. F. *Angew. Chem., Int. Ed.* **2002**, *41*, 2176.
(8) Xu, S. P.; Ji, X. H.; Xu, W. Q.; Li, X. L.; Wang, L. Y.; Bai, Y. B.; Zhao, B.; Ozaki, Y. *Analyst* **2004**, *129*, 63.
(9) Hirsch, L. R.; Jackson, J. B.; Lee, A.; Halas, N. J.; West, J. *Anal. Chem.* **2003**, *75*, 2377.
(10) Tang, D. P.; Yuan, R.; Chai, Y. Q.; Zhong, X.; Liu, Y.; Dai, J. Y.; Zhang, L. Y. *Anal. Biochem.* **2004**, *333*, 345.
(11) Liang, R. Q.; Tan, C. Y.; Ruan, K. C. *J. Immunol. Methods* **2004**, *285*, 157.
(12) Lee, K. B.; Kim, E. Y.; Mirkin, C. A.; Wolinsky, S. M. *Nano Lett.* **2004**, *4*, 1869.
(13) Nath, N.; Chilkoti, A. *Anal. Chem.* **2002**, *74*, 504.
(14) Su, X. D.; Li, S. F. Y.; O'Shea, S. J. *Chem. Commun.* **2001**, 755.
(15) Hirsch, L. R.; Stafford, R. J.; Bankson, J. A.; Sershen, S. R.; Rivera, B.; Price, R. E.; Hazle, J. D.; Halas, N. J.; West, J. L. *Proc. Natl. Acad. Sci. U.S.A.* **2003**, *100*, 13549.
(16) Elghanian, R.; Storhoff, J. J.; Mucic, R. C.; Letsinger, R. L.; Mirkin, C. A. *Science* **1997**, *277*, 1078.
(17) Taton, T. A.; Mirkin, C. A.; Letsinger, R. L. *Science* **2000**, *289*, 1757.
(18) Salem, A. K.; Searson, P. C.; Leong, K. W. *Nat. Mater.* **2003**, *2*, 668.
(19) Sershen, S. R.; Westcott, S. L.; Halas, N. J.; West, J. L. *J. Biomed. Mater. Res.* **2000**, *51*, 293.
(20) Mrksich, M. *Chem. Soc. Rev.* **2000**, *29*, 267.
(21) Connor, E. E.; Mwamuka, J.; Gole, A.; Murphy, C. J.; Wyatt, M. D. *Small* **2005**, *1*, 325.

10.1021/la051069t CCC: $30.25
Published on Web 08/26/2005

therapeutic agents can be encapsulated and/or conjugated onto the drug carriers which serve as sustained release systems to overcome problems such as poor solubility, low stability, poor biodistribution, and lack of selectivity.[23] Primarily, the materials suitable for DDS should be nontoxic. Furthermore, after drug carriers are fabricated, if applied in vivo, they should have a long circulating time in the body until they complete their "mission" after the administration. The surface can be modified with PEG to possess stealthy "coats" which can protect particulate DDS from clear-up by the immune system in the body defense so as to prolong the blood circulation time.[24,25] This explains why PEG is the most widely used among a variety of hydrophilic macromolecules for imparting hydrophilic surface character to the particulates.[26,27] In this paper, we report the effect of a gold layer of the nanosized spherical DDS on the cell cytotoxicity by evaluating the cell proliferation. The main frame of the structures employed here was constructed from two different copolymers including poly(L,L-lactide-*co*-ethylene glycol) (PLLA-PEG) and poly(*N*-isopropylacrylamide-*co*-D,D-lactide) (PNIPAAm-PDLA) via the modified double-emulsion method (MDEM), as reported earlier;[28] hereafter, this is abbreviated as PLLA-PEG@PNIPAAm-PDLA. Afterward, the surface of the PLLA-PEG@PNIPAAm-PDLA was functionalized by amino alkyl silane to attract Au nanoparticles so that PLLA-PEG@PNIPAAm-PDLA with a gold layer (Au@PLLA-PEG@PNIPAAm-PDLA) was fabricated. As the name denotes, a "shell-in-shell" structure comprises two shells: the inner shell of thermosensitive diblock copolymer, PNIPAAm-PDLA, and the outer shell of the biodegradable copolymer, PLLA-PEG. Its unique thermal response was confirmed by optical and thermal analysis, and the release rate of BSA encapsulated in Au@PLLA-PEG@PNIPAAm-PDLA was examined to evaluate its thermal dependence on the temperature, showing an increased release rate above the LCST. Most importantly, the cytotoxicities of Au@PLLA-PEG@PNIPAAm-PDLA and PLLA-PEG@PNIPAAm-PDLA were examined by testing with 3-(4,5-dimethylthiazol-2-yl)-5-(3-carboxymethoxyphenyl)-2-(4-sulfophenyl)-2*H*-tetrazolium (MTS) and two-color cell fluorescence viability (TCCV) assay with human cervical adenocarcinoma cells (HeLa cells) and transformed African green monkey kidney fibroblast cells (Cos-7 cells).

2. Experimental Section

2.1. Materials. D,D-Lactide (99.5%) and L,L-lactide (99.5%) were generously provided by PURAC Corporation (Gorinchem, The Netherlands). *N*-Isopropylacrylamide (NIPAAm, 98%), benzoyl peroxide (BPO, 40% blended in dibutyl phthalate), β-mercaptoethanol (99%), stannous 2-ethylhexanoate (98%), $HAuCl_4 \cdot 3H_2O$ (99%), trisodium citrate (TSC, 99%), sodium borohydride ($NaBH_4$, 99%), BSA (fraction V), PEG (M_w of 4 kDa), poly(vinyl alcohol) (PVA, M_w of 15 kDa), 3-aminopropyltrimethoxysilane (APTMS, 99.9%), sodium azide (99.99%), and the bicinchoninic acid (BCA) protein assay kit were purchased from Sigma-Aldrich chemicals. The LIVE/DEAD vitality/cytotoxicity kit, two-color cell fluorescence viability assay (TCCV), and CellTiter 96 AQueous One Solution cell proliferation assay were purchased from Promega Corp. (Wallisellen, Switzerland). Ammonium molybdate (99%) was purchased from KEBO chemicals (Stockholm, Sweden). Phosphate-buffered saline (PBS) tablets were purchased from Medicago AB (Uppsala, Sweden). The cellulose membrane bag (M_w cutoff: 100 kDa) was purchased from Spectrum Inc. (Breda, The Netherlands). All organic solvents were of reagent grade and used without further purification, and deionized water was obtained from Milli-Q system. All the cell media and supplements for cell experiments were purchased from Invitrogen AB (Basel, Switzerland).

Scheme 1. Synthetic Pathway of PNIPAAm-PDLA and PLLA-PEG Block Copolymers

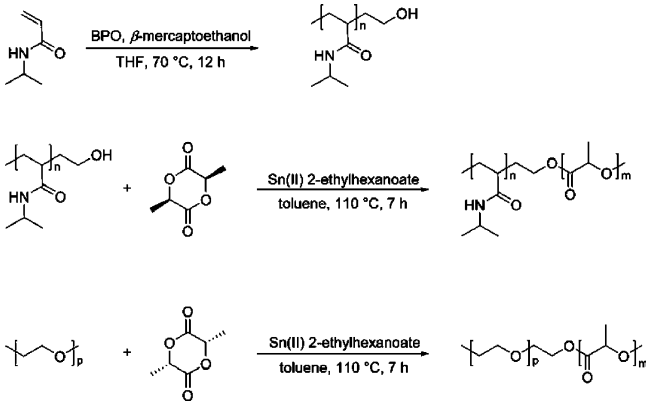

2.2. Characterization and Analysis. ^{1}H NMR spectra were recorded on a Bruker Avance-600 MHz spectrometer with $CDCl_3$ as the solvent. FT-IR spectra were recorded on a Nicolet Avatar 360 E. S. P. spectrophotometer equipped with a He−Ne laser and an MCT detector with 2 cm^{-1} resolution. Transmission electron microscopy (TEM) images were taken using a JEOL JEM-2000EX at an acceleration voltage of 200 kV. The particle size distribution was measured by a quasi-elastic light scattering (QELS) particle sizer (Brookhaven BI-90) equipped with a He−Ne laser beam (λ = 633 nm) at 20 °C. A Varian Cary 100 Bio UV−vis spectrophotometer was used to determine the LCST and quantitate the concentration of BSA by means of the BCA assay. The LCST was also confirmed by differential scanning calorimetry (DSC 2920, TA Instruments, Inc.)

2.3. Synthesis of PNIPAAm-PDLA and PLLA-PEG Diblock Copolymers. The diblock copolymers were synthesized according to the procedures reported previously.[28,29] The synthetic pathway is depicted in Scheme 1. Briefly, PNIPAAm was synthesized at 70 °C for 12 h via free radical polymerization under anhydrous conditions using tetrahydrofuran (THF) as the solvent. BPO (0.047 g) was used as an initiator and mixed with NIPAAm (5.01 g) and β-mercaptoethanol (0.11 g). Thereafter, synthesized PNIPAAm homopolymer (2.0 g), D,D-lactide (0.22 g), and stannous 2-ethylhexanoate (0.22 g) were mixed in anhydrous toluene, and the second synthesis was performed at 110 °C under nitrogen gas for 7 h. ^{1}H NMR ($CDCl_3$): δ = 1.14 (3H, PNIPAAm), 1.50 (2H, PNIPAAm), 1.58 (3H, PLA), 1.91 (1H, PNIPAAm), 3.97 (1H, PNIPAAm), 5.16 (1H, PLA). FT-IR (thin film): ν = 2970, 2940, and 2880 cm^{-1} (alkyl groups), 1750 cm^{-1} (carbonyl stretching-amide I), 1540 cm^{-1} (amide II), 1460 cm^{-1} (methyl groups), 1370 and 1390 cm^{-1} (isopropyl groups).

Parallelly, PLLA-PEG copolymer was synthesized from PEG, L,L-lactide, and stannous 2-ethylhexanoate in anhydrous toluene. The polymerization was carried out at 110 °C under nitrogen gas for 7 h. Upon completion of the reaction, polymer was collected by precipitating against an excess volume of cold diethyl ether. The solution was filtered off and dried in vacuo at an ambient temperature overnight. ^{1}H NMR ($CDCl_3$): δ = 1.58 (3H, PLA), 3.65 (2H, PEG), 5.16 (1H, PLA). FT-IR (thin film): ν = 2890 cm^{-1} ($-CH_2-$), 1760 cm^{-1} (C=O), 1130 and 1109 cm^{-1} (−C−O−C−), 2970 ($-CH_3$), 2940 cm^{-1} (−CH−).

2.4. Fabrication of PLLA-PEG@PNIPAAm-PDLA. An aqueous solution of BSA (330 μL, 8 wt %) was dropped into

(22) Langer, R. *Science* **1990**, *249*, 1527.
(23) Allen, T. M.; Cullis, P. R. *Science* **2004**, *303*, 1818.
(24) Gref, R.; Minamitake, Y.; Peracchia, M. T.; Trubetskoy, V.; Torchilin, V.; Langer, R. *Science* **1994**, *263*, 1600.
(25) Storm, G.; Belliot, S. O.; Daemen, T.; Lasic, D. D. *Adv. Drug Delivery Rev.* **1995**, *17*, 31.
(26) Araujo, L.; Lobenberg, R.; Kreuter, J. *J. Drug Targeting* **1999**, *6*, 373.
(27) Gaur, U.; Sahoo, S. K.; De, T. K.; Ghosh, P. C.; Maitra, A.; Ghosh, P. K. *Int. J. Pharm.* **2000**, *202*, 1.
(28) Jo, Y. S.; Kim, D. K.; Jeong, Y. K.; Kim, K. J.; Muhammed, M. *Macromol. Rapid Commun.* **2003**, *24*, 957.
(29) Jo, Y. S.; Kim, M. C.; Kim, D. K.; Kim, C. J.; Jeong, Y. K.; Kim, K. J.; Muhammed, M. *Nanotechnology* **2004**, *15*, 1186.

Scheme 2. Evolution of Au@PLLA-PEG@PNIPAAm-PDLA

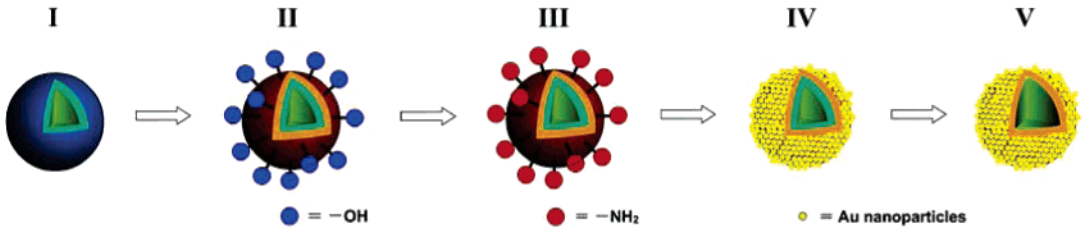

(I) Formation of the BSA-loaded PNIPAAm-PDLA nanospheres. (II) Construction of the PLLA-PEG@PNIPAAm-PDLA dual-shell structure by an MDEM. (III) Functionalization of the PLLA-PEG@PNIPAAm-PDLA dual-shell structure with APTMS. (IV) Immobilization of Au nanoparticles on the surface of PLLA-PEG@PNIPAAm-PDLA. (V) Elimination of the inner shell when the temperature is above the LCST.

chloroform containing PNIPAAm-PDLA diblock copolymer (3 mL, 4 wt %) followed by sonication in an ice bath for 2 min. Consequently, a "water-in-oil" (W/O) emulsion was formed. Afterward, the W/O emulsion (160 μL) was mixed with the PLLA-PEG chloroform solution (160 μL, 4 wt %) and added dropwise to PVA aqueous solution (3 mL, 0.6 wt %) followed by sonication in an ice bath for another 2 min.

2.5. Fabrication of Au@PLLA-PEG@PNIPAAm-PDLA. The silanization was carried out by mixing the emulsion of PLLA-PEG@PNIPAAm-PDLA with APTMS-containing ethanol (160 μL, 1 wt %) in order to functionalize the surface of the nanospheres with amino groups. Colloidal gold nanoparticles were synthesized by reducing $[AuCl_4]^-$ ions in the presence of a reductant, $NaBH_4$. The detailed procedure is described elsewhere.[30] After the silanization, gold colloid suspension (10 mL) was added dropwise into the amino-modified PLLA-PEG@PNIPAAm-PDLA emulsion with vigorous agitation for 15 min. The mixture was maintained at room temperature for another 30 min.

2.6. BSA Release Test. In vitro release profiles were obtained as follows. An appropriate amount of BSA-loaded Au@PLLA-PEG@PNIPAAm-PDLA was introduced into a dialysis membrane bag and placed in 100 mL of PBS as a media containing 0.02 wt % sodium azide. Two comparative experiments were simultaneously undertaken, one at 22 °C as a control and the other at 37 °C. At the predetermined time intervals, 0.5 mL aliquots of the aqueous solution were withdrawn from the media and the protein quantity was analyzed by BCA assay.[31,32]

2.7. Cell Viability Test. PLLA-PEG@PNIPAAm-PDLA and Au@PLLA-PEG@PNIPAAm-PDLA were dialyzed with cellulose membrane (M_w cutoff: 3 kDa) against water for 48 h and then lyophilized for 72 h. Stock solutions were prepared at the concentration of 20 mg/mL. Four different concentrations of the solutions were sequentially prepared by diluting the stock solution with the appropriate amount of cell media.

2.7.1. Cell Line and Cell Culture. HeLa cells (human cervical epithelial carcinoma cell line) and Cos-7 cells (African green monkey kidney cell line) were purchased from American Type Culture Collection (ATCC). HeLa cells and Cos-7 cells were cultured in complete media (MEM-α or DMEM) containing 10% fetal bovine serum (FBS) and 1% of antibiotic/antimycine at 37 °C in a humidified 5% CO_2 -containing atmosphere.

2.7.2. MTS Assay. Cells were prepared at a density of 5×10^4 cells mL^{-1} of medium. The prepared cells were seeded 200 μL in each well of a 96-well microplate. The cells were incubated for 24 h prior to polymer addition. The cells were incubated with various concentrations of polymer for 48 h. The medium was removed and replaced with 100 μL of growth medium prior to the addition of the 20 μL/well of CellTiter 96 AQueous One Solution reagent based on the MTS assay. After the plate was incubated for 4 h at 37 °C, the plates were read using an ELISA reader at a test wavelength of 570 nm and a reference wavelength of 630 nm. The result was expressed relative to results from untreated cells. Untreated cells were used as a positive control. The medium without cells was used as a blank.

The cell viability (%) was calculated according to the following equation:

$$\text{Cell viability (\%)} = (OD_{sample} - OD_{blank})/(OD_{control} - OD_{blank}) \times 100$$

2.7.3. TCCV Assay. Cells were seeded on 6-well glass plates. Aspirating cell media from the wells, they were filled with the working solution prepared by mixing 2 μL of 2 mM ethidium homodimer-1 solution diluted in 1 mL of PBS with 0.5 μL of calcein AM solution. The glass plates were incubated in darkness for 30 min. The wells were washed with PBS twice and filled with 1 mL of PBS per well after the contained solutions were aspirated. Images were taken by an Axio Vert 200M fluorescence microscope (Carl Zeiss Inc., Thornwood, NY).

3. Results and Discussion

3.1. PLLA-PEG@PNIPAAm-PDLA and Au@PLLA-PEG@PNIPAAm-PDLA. Poly(*N*-isopropylacrylamide) (PNIPAAm) undergoes a sharp and reversible phase transition at a specific lower critical solubility temperature (LCST).[33−45] Up to now, a wide variety of medical implements made from PNIPAAm have been proposed in different forms, e.g., micelles,[34,35] nanoparticles,[36] hydrogel,[37] and tablets.[38] Not only PNIPAAm homopolymer itself, but the applications have also been expanded to other PNIPAAm derivative materials in combination with organic/inorganic counterparts such as PNIPAAm-poly(butyl methacrylate),[34] PNIPAAm-poly(D,L-lactide),[35] PNIPAAm-polystyrene,[41] and Ag-PNIPAAm-polystyrene.[46] Scheme 2 illustrates the evolution pathway in constructing Au@PLLA-PEG@PNIPAAm-PDLA. To serve as a constituent for the vehicles to load BSA inside,

(30) Grabar, K. C.; Allison, K. J.; Baker, B. E.; Bright, R. M.; Brown, K. R.; Freeman, R. G.; Fox, A. P.; Keating, C. D.; Musick, M. D.; Natan, M. J. *Langmuir* **1996**, *12*, 2353.
(31) Smith, P. K.; Krohn, R. I.; Hermanson, G. T.; Mallia, A. K.; Gartner, F. H.; Provenzano, M. D.; Fujimoto, E. K.; Goeke, N. M.; Olson, B. J.; Klenk, D. C. *Anal. Biochem.* **1985**, *150*, 76.
(32) Wiechelman, K. J.; Braun, R. D.; Fitzpatrick, J. D. *Anal. Biochem.* **1988**, *175*, 231.
(33) Topp, M. D. C.; Dijkstra, P. J.; Talsma, H.; Feijen, J. *Macromolecules* **1997**, *30*, 8518.
(34) Chung, J. E.; Yokoyama, M.; Suzuki, K.; Aoyagi, T.; Sakurai, Y.; Okano, T. *Colloids Surf., B* **1997**, *9*, 37.
(35) Kohori, F.; Sakai, K.; Aoyagi, T.; Yokoyama, M.; Sakurai, Y.; Okano, T. *J. Controlled Release* **1998**, *55*, 87.
(36) Sakuma, S.; Suzuki, N.; Kikuchi, H.; Hiwatari, K.; Arikawa, K.; Kishida, A.; Akashi, M. *Int. J. Pharm.* **1997**, *149*, 93.
(37) Okubo, T.; Hase, H.; Kimura, H.; Kokufutat, E. *Langmuir* **2002**, *18*, 6783.
(38) Yuk, S. H.; Cho, S. H.; Lee, S. H. *Macromolecules* **1997**, *30*, 6856.
(39) Eeckman, F.; Moes, A. J.; Amighi, K. *J. Controlled Release* **2003**, *88*, 105.
(40) Eeckman, F.; Moes, A. J.; Amighi, K. *Int. J. Pharm.* **2002**, *241*, 113.
(41) Cammas, S.; Suzuki, K.; Sone, C.; Sakurai, Y.; Kataoka, K.; Okano, T. *J. Controlled Release* **1997**, *48*, 157.
(42) Chung, J. E.; Yokoyama, M.; Okano, T. *J. Controlled Release* **2000**, *65*, 93.
(43) Chung, J. E.; Yokoyama, M.; Yamato, M.; Aoyagi, T.; Sakurai, Y.; Okano, T. *J. Controlled Release* **1999**, *62*, 115.
(44) Demanuele, A.; Dinarvand, R. *Int. J. Pharm.* **1995**, *118*, 237.
(45) Kim, I. S.; Jeong, Y. I.; Cho, C. S.; Kim, S. H. *Int. J. Pharm.* **2000**, *211*, 1.
(46) Chen, C. W.; Chen, M. Q.; Serizawa, T.; Akashi, M. *Adv. Mater.* **1998**, *10*, 1122.

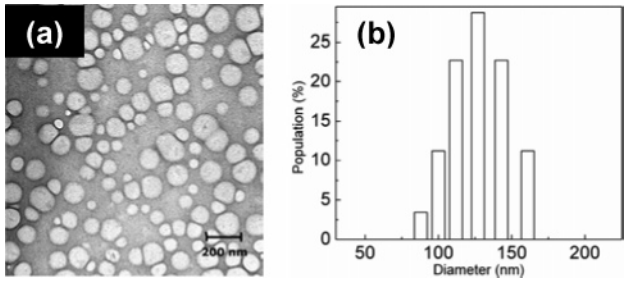

Figure 1. (a) TEM image of PLLA-PEG@PNIPAAm-PDLA (negatively stained with 2% aqueous ammonium molybdate solution for 2 min) and (b) particle size distribution of the PLLA-PEG@PNIPAAm-PDLA nanospheres.

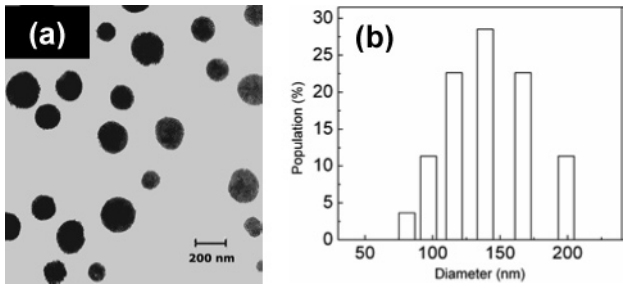

Figure 2. (a) TEM image of Au@PLLA-PEG@PNIPAAm-PDLA (without staining) and (b) particle size distribution of the Au@PLLA-PEG@PNIPAAm-PDLA nanospheres.

Au@PLLA-PEG@PNIPAAm-PDLA is in the form of a dual-shell vesicle fabricated by MDEM. Hydroxyl groups on the surface of PLLA-PEG@PNIPAAm-PDLA are functionalized into amino groups, and gold nanoparticles are deposited to form Au@PLLA-PEG@PNIPAAm-PDLA (Steps I−IV). Above the LCST, this allows BSA molecules to be released out at an elevated temperature through a single outer shell ultimately, because thermosensitive inner shells are designed to be burst and eliminated (Step V). The resulting nanoparticles are well-defined as shown in Figures 1 and 2, along with the information of the size and polydispersity index.

The size distribution of PLLA-PEG@PNIPAAm-PDLA lies in the range of 80−170 nm, confirmed by the QELS particle sizer. The mean diameter of PLLA-PEG@PNIPAAm-PDLA is 127 nm with a polydispersity index of 1.41. Gold layers constructed with gold nanoparticles are clearly seen on Au@PLLA-PEG@PNIPAAm-PDLA as dark spots in Figure 2a. It is noted that the particle size slightly increases up to 140 nm compared to that of PLLA-PEG@PNIPAAm-PDLA. This size change results from the decreased mobility due to gold nanoparticles' deposition, which is reflected in calculating the mean diameter by the QELS particle sizer.

3.2. Determination of the LCST. The LCST of PNIPAAm-PDLA copolymer is observed at 36.7 °C from a sharp endothermic peak in the DSC curve. However, no significant endo/exothermic peak of PLLA-PEG appears in the same temperature range (Figure 3). This reflects that the PNIPAAm-PDLA copolymer undergoes a phase transition at the LCST, 36.7 °C. As for the analysis by UV−vis spectrometry, an aqueous solution of PNIPAAm-PDLA is transparent at temperatures lower than the LCST. However, as the temperature increases, the solution becomes turbid and the transmittance rate, as shown in Figure 4, trace a, decreases in a sigmoidal shape owing to the predominant hydrophobicity over the hydrophilicity driven by the phase transition. From this graph, the maximum corresponding to the LCST of PNIPAAm-PDLA is found from the numerically differentiated curve

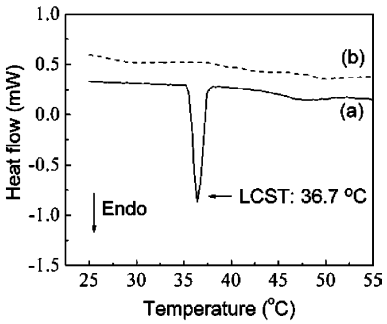

Figure 3. DSC data obtained from PNIPAAm-PDLA (trace a) and PLLA-PEG (trace b).

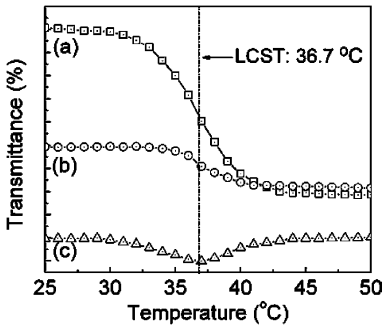

Figure 4. Visible transmittance at 500 nm: transparency change of the PNIPAAm-PDLA solution (trace a); transparency change of Au@PLLA-PEG@PNIPAAm-PDLA in W/O/W emulsion (trace b); a differentiated curve of trace a (trace c).

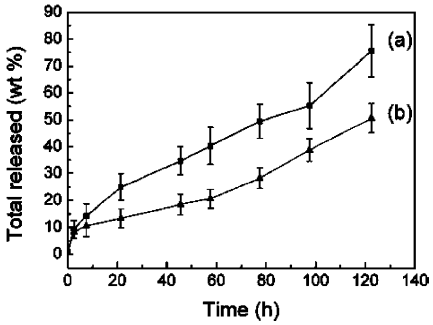

Figure 5. In vitro release profiles of BSA from Au@PLLA-PEG@PNIPAAm-PDLA in pH 7.4 PBS solution: trace a, 37 °C; trace b, 22 °C.

of the transmittance rate, revealing the LCST at 36.7 °C (Figure 4, trace c). This temperature is not only the same as that obtained by DSC, but is also equal to the human body temperature. Parallelly, it is observed that the transmittance rate of the emulsion containing Au@PLLA-PEG@PNIPAAm-PDLA also decreases in the same fashion as temperature increases (Figure 4, trace b). While the transparency of the PNIPAAm-PDLA solution is reversibly regained in the case where the solution is cooled to ambient temperature, the transmittance rate of Au@PLLA-PEG@PNIPAAm-PDLA is not restored, suggesting that the thermosensitive inner shell of the Au@PLLA-PEG@PNIPAAm-PDLA is irreversibly disrupted once PNIPAAm-PDLA undergoes the phase transition by thermal stimulus above the LCST.

3.3. BSA Release Test. BSA release rates are monitored at two different temperatures including ambient temperature and human body temperature. The results are demonstrated in Figure 5 by plotting the released amount of BSA versus time. The percentage of total BSA amount released, represented on the *y*-axis, is calculated based on the maximum amount of BSA under the

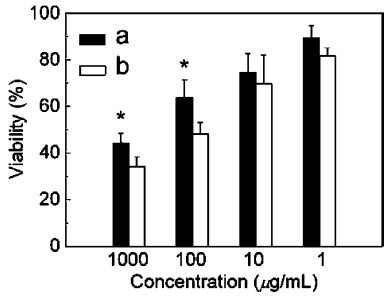

Figure 6. MTS assay using the HeLa cell line after incubation with Au@PLLA-PEG@PNIPAAm-PDLA (solid bars labeled a) and PLLA-PEG@PNIPAAm-PDLA (open bars labeled b) for 2 days. (The asterisks denote $p < 0.05$ by the Student's t test.)

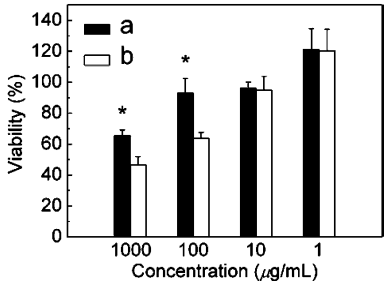

Figure 7. MTS assay using the Cos-7 cell line after incubation with Au@PLLA-PEG@PNIPAAm-PDLA (solid bars labeled a) and PLLA-PEG@PNIPAAm-PDLA (open bars labeled b) for 2 days. (The asterisks denote $p < 0.05$ by the Student's t test.)

assumption that all the BSA molecules would be ultimately diffused out without any other chemical reaction between the BSA molecules and the polymeric chains in the experimental system. In Figure 5, the two curves represent different release rates, respectively. In the two different profiles, the profile at 37 °C (Figure 5, trace a) shows a quasi-linear increase in the release rate of BSA; however, the release rate at 22 °C (Figure 5, trace b) increases smoothly before 60 h and expedites thereafter, caused by induced instability of the dual-shell structure, while the profile at 37 °C maintains the high release rate, which can be attributed to the disrupted inner shell. Therefore, the inner shell bursting above the LCST causes the main difference in the release rates, because as the temperature is elevated above the LCST, the inner shell becomes unstable, and the dual-shell structure changes into a simple single-shell structure. In this stage, the release rate will be dominated only by various parameters involving PLLA-PEG, the component of the outer shell. Then, the ongoing release behavior follows the release mechanism from the single-shell structure. In general, several factors are suggested to determine the release rate of a drug from polymeric carriers, e.g., diffusion through the polymeric matrix, dissolution of the drug, polymer degradation, etc.[29]

3.4. Cytotoxicity Evaluation. In Figures 6 and 7, MTS assay results indicate that neither of the nanospheres exerts any critical influence on either of the cells. In addition, dead/living cells are visualized as fluorescent microscope images taken after the TCCV assay. No remarkable effect on the cell morphology and viability is observed. As seen in Figures 8 and 9, the majority of the cells are alive with no significant destructive effect in both cases (Au@PLLA-PEG@PNIPAAm-PDLA and PLLA-PEG@PNIPAAm-PDLA).

It is noticeable that, although the cell viability of PLLA-PEG@PNIPAAm-PDLA is to some extent lower than that of Au@PLLA-PEG@PNIPAAm-PDLA, still excellent bio-

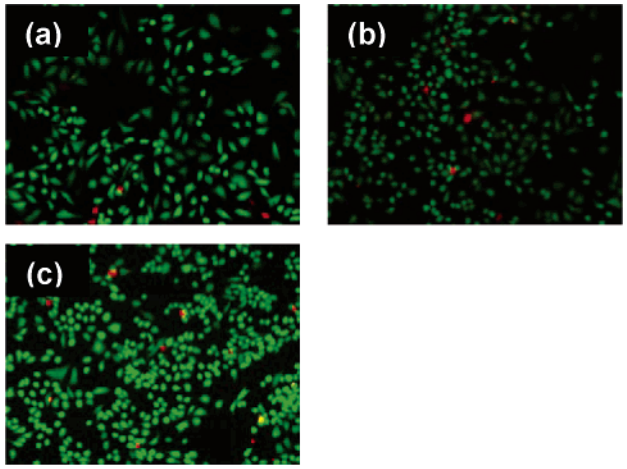

Figure 8. Fluorescence microscopy images of HeLa cells exposed to (a) 100 μg/mL Au@PLLA-PEG@PNIPAAm-PDLA nanospheres, (b) 1000 μg/mL PLLA-PEG@PNIPAAm-PDLA nanospheres, and (c) the control, where the green spots represent living cells and the red ones represent dead cells.

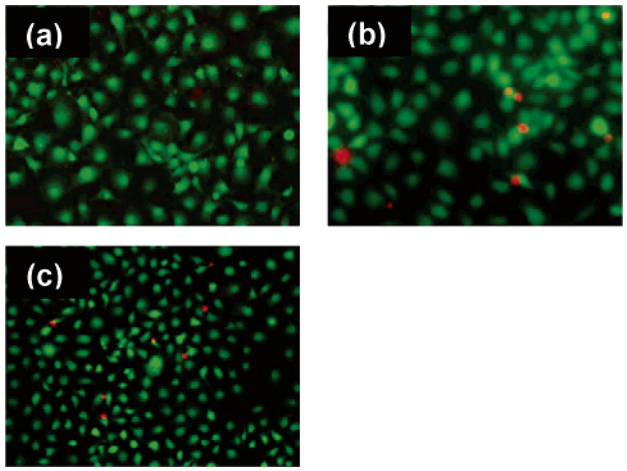

Figure 9. Fluorescence microscopy images of Cos-7 cells exposed to (a) 1000 μg/mL Au@PLLA-PEG@PNIPAAm-PDLA nanospheres, (b) 1000 μg/mL PLLA-PEG@PNIPAAm-PDLA nanospheres, and (c) the control, where the green spots represent living cells and the red ones represent dead cells.

compatibility is acquired. At lower doses of 10 and 1μg/mL, the cell viability of PLLA-PEG@PNIPAAm-PDLA reaches as high as 70% (HeLa cells) and even higher than 90% (Cos-7 cells), which is almost comparable to Au@PLLA-PEG@PNIPAAm-PDLA. However, interestingly, Au@PLLA-PEG@PNIPAAm-PDLA exhibits significantly enhanced cell viability even at high doses such as 1000 μg/mL and 100 μg/mL in a 48 h incubation ($p < 0.05$). This effect contributed by the gold layer is commonly observed in both cells. It suggests that the beneficial effect of the gold layer is predominantly maximized especially at high doses.

In our study, no receptor-mediated endocytosis is proposed, and a large portion of the nanospheres is unlikely to be internalized because no favorable size effect exists for endocytosis. Consequently, there is no driving force to ameliorate or deteriorate cell proliferation taking place in the cytoplasm. Nonetheless, PLLA-PEG diblock copolymer as the outer shell component of PLLA-PEG@PNIPAAm-PDLA is presumed to reduce the interfacial affinity between "foreign" spheres and protein molecules due to its hydrophilicity. The PEG constituent does not merely play a role in preventing the particles from being anchored by proteins, but more importantly,

it diminishes the opportunity of the nanospheres to attach to the cell membrane which may be induced by various interactions. In contrast, gold possesses a high affinity to biomacromolecules including various immunoglobulins, albumins, and fibrinogen residing in vivo conditions in comparison to a hydroxylated surface.[47] Likewise, the exterior gold layer of Au@ PLLA-PEG@PNIPAAm-PDLA is, at the first stage, supposedly coated with a variety of proteins in the cell media, whereas PLLA-PEG@PNIPAAm-PDLA does not undergo the same binding process. In the next stage, therefore, Au@PLLA-PEG@PNIPAAm-PDLA surrounded by the proteins initiates the interaction with the surface of the cell membrane. It is another key to explain how cell proliferation can be promoted by accelerated transport of nutrients from media into cytoplasm. Moreover, Au@PLLA-PEG@PNIPAAm-PDLA anchored on the cell membrane may lower the potential in transmembrane uptake and facilitate the diffusion rate of nutrient penetrating through the cell membrane. Because most cells take up nutrients such as lipids from the medium of in vitro cell-culturing conditions, this action can be also explained by the physiological interaction between proteins and fatty acids/phospholipids in cellular membranes as a result of the membrane disruption.[48,49]

4. Conclusions

Following successful fabrication of the BSA-loaded "shell-in-shell" nanospheres by an MDEM, gold nanoparticles are immobilized on the surface by functionalization of terminal groups of PEG chains. Protein release behavior is also monitored, and a significant difference between the two releasing profiles reveals the thermal dependence due to the inner shell bursting when the temperature is elevated higher than the LCST, 36.7 °C as determined. With a similar platform of spherical nanostructures, the gold layer gives better enhanced biocompatibility especially at a high dose of polymeric nanospheres. This is explained by the interfacial action between the exterior of the cell membrane and protein molecules adsorbed on the gold layer which may play a crucial role of attracting the nanospheres onto the cellular membrane and successively promoting the transport of essential substances for cellular metabolism by transmembrane uptake.

Acknowledgment. The authors are grateful to Dr. M. S. Toprak for help with the synthesis of the Au nanoparticles and other valuable technical support. We appreciate the help from Dr. M. Mikhaylova for critically reading the manuscript and providing fruitful advice.

LA051069T

(47) Kalltorp, M.; Carlen, A.; Thomsen, P.; Olsson, J.; Tengvall, P. *J. Mater. Sci.: Mater. Med.* **2000**, *11*, 191.

(48) Martinez-Cayuela, M.; Garcia-Pelayo, M. C.; Linares, A.; Garcia-Peregrin, E. *J. Biochem.* **2000**, *128*, 545.

(49) Hamilton, J. A. *J. Lipid Res.* **1998**, *39*, 467.